Modelling and Experimental Verification of an Unglazed Metal Façade Collector Model

Viacheslav Shemelin and Tomas Matuska

Czech Technical University in Prague, University Centre for Energy Efficient Buildings, 27343, Bustehrad, Czech Republic

Abstract

The paper presents a theoretical model for energy performance simulation of an unglazed metal façade collector (UMFC). Different configurations of UMFC were developed and experimentally tested with the use of an indoor solar simulator to perform a verification process. The verification of the model demonstrated that there is a good agreement between the simulated and experimentally obtained results. The sensitivity analysis has been performed to demonstrate the influence of the wind-forced convection model on the theoretically calculated efficiency. However, the results of the analysis indicated that it is extremely important to identify an appropriate wind-forced convection correlation for the estimation of the thermal performance of a UMFC. A large number of correlations for wind-forced convection presented in the literature demonstrated that there is no universally acceptable correlation. The difference was caused by different combinations of experimental and operating conditions (ambient air temperature, wind range, wind tunnel/outdoor/indoor measurement, instrumentation, surroundings, etc.). Therefore, it was highly recommended to provide a long-term verification process of the model since the climatic and operating conditions (especially wind-related conditions for instance wind speed, wind direction, wind turbulence, etc.) are different compared to an indoor verification process.

Keywords: Unglazed solar thermal collector, metal façade cladding system, building integrated solar thermal (BIST), wind-forced convection

1. Introduction

The utilization of solar energy using a building envelope becomes more and more attractive today. It offers great environmental benefits (reduction in primary energy consumption, reduction in greenhouse gas emissions, etc.) as well as economic benefits (reduction in building operating costs, sustainable operation, public subsidies, etc.). Particularly the usage of efficient, technically reliable, and time-proven solar thermal technologies has great potential. Among solar thermal technologies, unglazed solar thermal collectors have lower thermal performance compared to glazed flat-plate collectors or vacuum tube collectors. Unglazed solar thermal collectors for a long time were utilized primarily for low operation temperature heating purposes in applications such as swimming pool heating or as an evaporator in a heat pump system. The high magnitude of heat losses (mainly caused by convection) prevented their wider distribution in solar thermal applications. On the other hand, they are cheaper, lighter, and more reliable. Therefore, the combination of an unglazed solar thermal collector and a metal facade cladding system comes to mind. Such an unglazed metal façade collector (UMFC) is based on one key element (solar absorber metal sheet). Moreover, this solution brings a few advantages. Firstly, the metal cladding system is a well-established technology used by architects for new buildings, as well as for retrofit purposes. So, there is a large application potential. Secondly, a commercially available metal cladding system is available in a large palette of colours. It allows us to solve the aesthetic issues associated with the solar thermal integration processes. Thirdly, installing a UMFC system is faster than an entirely new façade solution because UMFC is based on a commercially available metal cladding system. Last but not least, the energy-active large-area building façade system can be used for direct hot water preparation and distribution, space heating in combination with a heat pump, direct space cooling (night radiative cooling), or space cooling in combination with a heat pump. It is, therefore, not surprising that metal unglazed solar thermal façade collector attracts attention from the scientific field (Probst and Roecker, 2007; Hermann et al., 2010; Giovanardi et al., 2015; Shen et al., 2016; Martinez et al., 2017; Weiland et al., 2019; Shemelin and Matuska, 2022).

doi:10.18086/eurosun.2022.12.15 Available at http://proceedings.ises.org

Analyzing the thermal performance of a UMFC is essential as it helps to improve the design. In fact, research and sensitivity analysis of design changes should be performed simultaneously to create an efficient device. Since the experimental study of all possible collector designs is not feasible, analytical methods such as computational modelling using a mathematical model must be employed. The benefits of computational modelling are the ability to study the thermal performance under different climatic and operating conditions which are difficult or impossible to create in laboratory conditions, to provide design changes sensitivity analysis, etc.

In the past, some studies investigated an unglazed thermal collector energy performance to create a mathematical model. For instance, Keller (1985) concluded that the significant difference in thermal performance modelling of glazed and unglazed solar thermal collectors is that the thermal performance of unglazed collectors is strongly influenced by six environmental factors (namely solar irradiance, ambient air temperature, longwave radiation, wind speed, rain, and condensation/frost.) while the thermal performance of glazed collectors primarily depends on only two environmental factors (solar irradiance and ambient air temperature). Later Morrison and Gilliaert (1992) modified the well-known Hottel-Whillier-Bliss equation (Bliss Jr., 1959; Hottel and Whillier, 1955; Hottel and Woertz, 1942; Whillier, 1967) for unglazed solar thermal collectors. It includes an allowance for longwave sky radiation and wind speed on the calculated thermal performance. Then Eisenmann et al. (2006) developed, experimentally validated, and described an additional energy gain of an unglazed metal collector, including the condensation phenomena. The condensation effect on a metal unglazed solar thermal collector heat gains was investigated and considered in several other collector models reported by (Morrison, 1994; Perers, 2010; Soltau, 1992; Stegmann et al., 2011). Later Anderson et al. (2013) investigated theoretically and experimentally the thermal performance of an unglazed thermal collector for radiant cooling. Bunea et al. (2015) developed and evaluated an unglazed solar thermal collector considering condensation/evaporation, frost/melting, and rain phenomena.

The proposed mathematical model aims best to represent the thermal behaviour under different design changes and quantify their influence on the collector's thermal performance. The presented model is a very detailed theoretical model with 17 input design parameters such as the absorber length, width, pipe thermal conductivity, bond material thermal conductivity, etc. It allows to perform a sensitivity analysis of design parameters under different climatic and operating conductions and to demonstrate their impact on the annual performance of UMFC-based solar systems. Moreover, this study outlines the influence of wind-forced heat transfer on thermal performance and indicates the importance of choosing an appropriate correlation for wind-forced convection.

2. Mathematical model

The proposed model is a detailed theoretical model of an unglazed metal façade liquid collector (see Fig. 1) that requires the geometrical (length of the metal absorber, width of the absorber, etc.), physical parameters (the metal absorber thermal conductivity, the pipe thermal conductivity, etc.), operating conditions (the collector heat transfer fluid mass flow rate, the collector heat transfer fluid inlet temperature, etc.) and climatic conditions (solar irradiance, ambient air temperature, wind velocity, etc.) to calculate the model outputs (the usable heat output, with respect to the collector area, and output heat transfer fluid temperature).

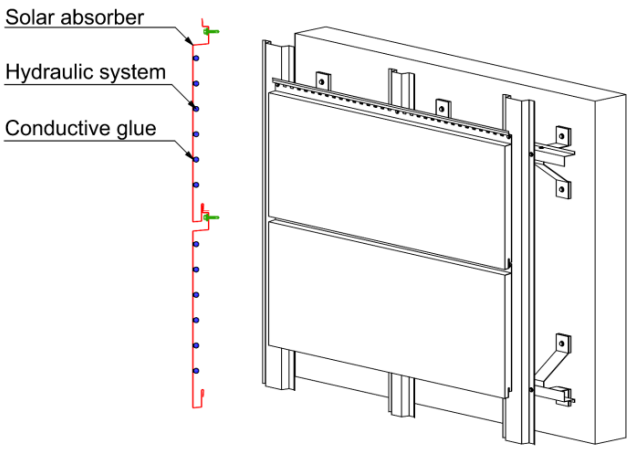

Fig. 1: The schematic layout of UMFC

The model uses the well-known one-dimensional useful energy output equation proposed by Hottel and Woertz (1942), Hottel and Whillier (1955) and Bliss Jr. (1959) so that

$$Q_{c,u} = A_{abs} F_R [\tau\alpha G - U(T_{in} - T_a)] \qquad \text{(eq. 1)}$$

where A_{abs} is the solar collector absorber area (m^2), F_R is the collector heat removal factor (-), τ is the solar transmittance of the collector cover, in the case of an unglazed solar collector it is equal to 1 (-), G is the global solar irradiance on the collector plane (W m^{-2}), U the collector overall heat loss coefficient (W m^{-2} K^{-1}), T_{in} is the heat transfer fluid inlet temperature (K), and T_a is the ambient air temperature (K).

In this equation, the fundamental difficulty is that there are two interdependent variables, the collector overall heat loss coefficient U and the collector heat removal factor F_R. The iteration cycle is introduced into the calculation process to solve this issue. In the first iteration step, the absorber T_{abs} and the heat transfer fluid T_{fluid} temperatures are estimated based on the inlet heat transfer fluid temperature T_{in}. Then, external and internal energy balances are calculated, describing the heat transfer process from the absorber surface to the surroundings and from the absorber surface to the heat transfer fluid, respectively. After that, the useful energy output is calculated according to Eq. (1). Afterwards, both estimated temperatures are recalculated. Finally, the recalculated absorber temperature T_{abs} and the heat transfer fluid temperature T_{fluid} are compared with the initial values. The calculation process continues as long as both temperatures are equal with 0.05 K difference. Typically, it takes from 3 to 5 iteration steps.

As mentioned above, the external energy balance describes the energy losses from the absorber surface to the surroundings. In the case of a UMFC, the external energy balance (see Fig. 2) consists of:

- the heat transfer processes by combined convection (forced and natural) and radiation from the front absorber surface to the ambient;
- the heat transfer processes by natural convection and radiation in the air gap between the back absorber surface and a façade wall.

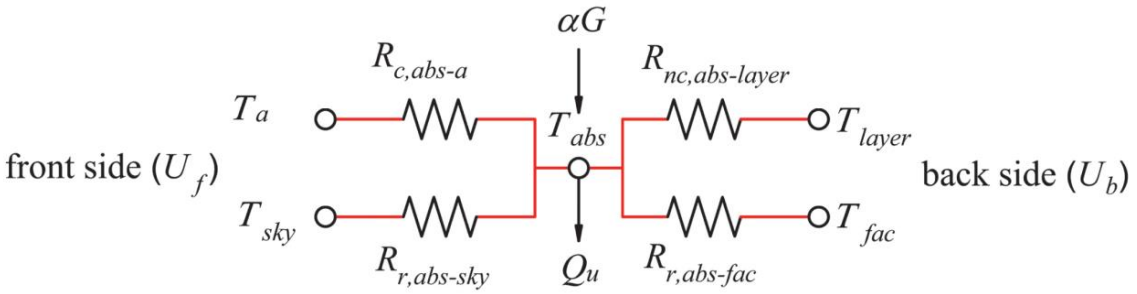

Fig. 2: Schematic layout of the external energy balance

To calculate the actual intensity of the heat transfer processes mentioned above, the absorber temperature T_{abs} should be known. On the other hand, the absorber temperature T_{abs} is dependent on the intensity of the heat transfer processes. Therefore, the absorber temperature T_{abs} in the first iteration step is estimated based on the heat transfer fluid inlet temperature T_{in}. Afterwards, the intensity of the heat transfer processes and the collector overall heat loss coefficient U are calculated based on the estimated absorber temperature T_{abs}.

The internal energy balance (see Fig. 3), contrary to the external energy balance, expresses the heat transfer processes inside a collector, from the absorber surface to the heat transfer fluid. It includes:

- the heat transfer process by fin conduction;
- the heat transfer process by bond conduction;
- the heat transfer process by pipe conduction;
- the heat transfer process by forced convection from the pipe surface to the heat transfer fluid.

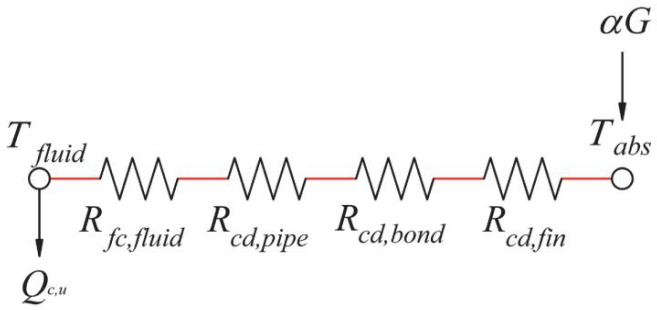

Fig. 3: Schematic layout of the internal energy balance

Here the situation here is very similar to the external energy balance. To calculate the actual intensity of the heat transfer processes, the heat transfer fluid mean temperature T_{fluid} should be known. On the other hand, the mean temperature of heat transfer fluid T_{fluid} is dependent on the intensity of the heat transfer processes. Hence, similar to external energy balance, in the first iteration step the heat transfer fluid mean temperature T_{fluid} is estimated based on the heat transfer fluid inlet temperature T_{in}. Then, the intensity of the heat transfer processes and the collector useful energy output $Q_{c,u}$ are determined based on the mean temperature of heat transfer fluid T_{fluid}.

3. Model verification

The proposed model was experimentally verified in Solar Laboratory operated under the University Centre for Energy Efficient Buildings (UCEEB) Czech Technical University in Prague. Ten UMFC prototypes different in design were produced using a commercially available metal cladding system to verify the model. Each prototype consists of a metal solar absorber with a solar absorptance α of 0.95, a longwave emittance ε of 0.95 and a hydraulic system (serpentine tube) bonded to the metal absorber sheet using conductive glue. The combinations of two pipe materials, three types of glue, three distances between pipes, and two prototype dimensions were used to demonstrate the performance sensitivity to different design parameters. A general dimensional scheme of the designed prototypes is illustrated in Fig. 4. The design parameters of the produced UMFC prototypes are presented in Tab. 1. The photos of the first experimental prototype are shown in Fig. 5.

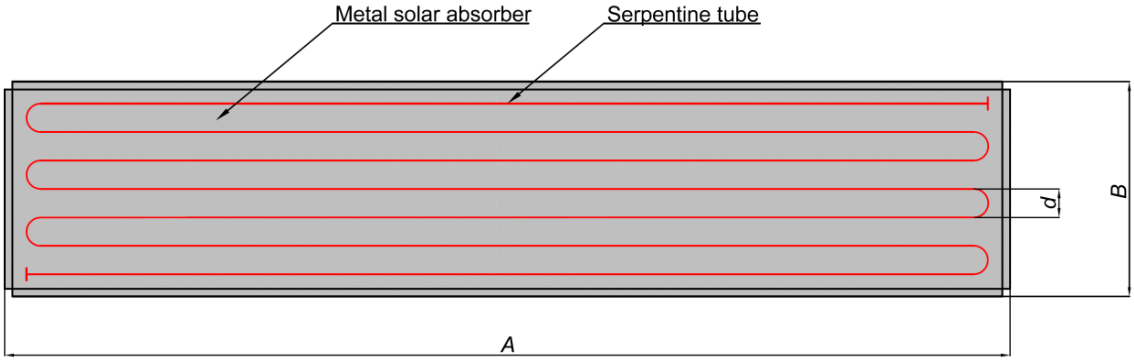

Fig. 4: The general dimensional scheme of the designed prototypes

Tab. 1: Design parameters of the produced UMFC prototypes

Prototype	Absorber material	Bond thermal conductivity (W m^{-1} K^{-1})	Distance between tubes d (mm)	Tube material	Absorber dimensions A x B (mm x mm)
1	Aluminium	2.8	90	Cu 15x1	2000 x 470
2	Aluminium	2.8	90	PEX 16x2	2000 x 470
3	Steel	1.4	90	PEX 16x2	2000 x 470
4	Steel	0.28	150	Cu 15x1	2000 x 470
5	Steel	0.28	150	PEX 16x2	2000 x 470

Tab. 1: Design parameters of the produced UMFC prototypes *(continued)*

6	Aluminium	1.4	90	PEX 16x2	3200 x 650
7	Aluminium	0.28	130	PEX 16x2	3200 x 650
8	Steel	1.4	130	Cu 15x1	3200 x 650
9	Steel	0.28	90	PEX 16x2	3200 x 650
10	Steel	0.28	130	PEX 16x2	3200 x 650

Fig. 5: Photos of the first experimental prototype

The produced prototypes were experimentally tested under stable climatic (solar irradiance, ambient air temperature, wind speed) and operating conditions (heat transfer fluid inlet temperature, heat transfer fluid flow rate) to determine the steady-state thermal output with the use of an indoor solar simulator (see Fig. 6 and Fig. 7). The sensors' type and their accuracy are given in Tab. 2.

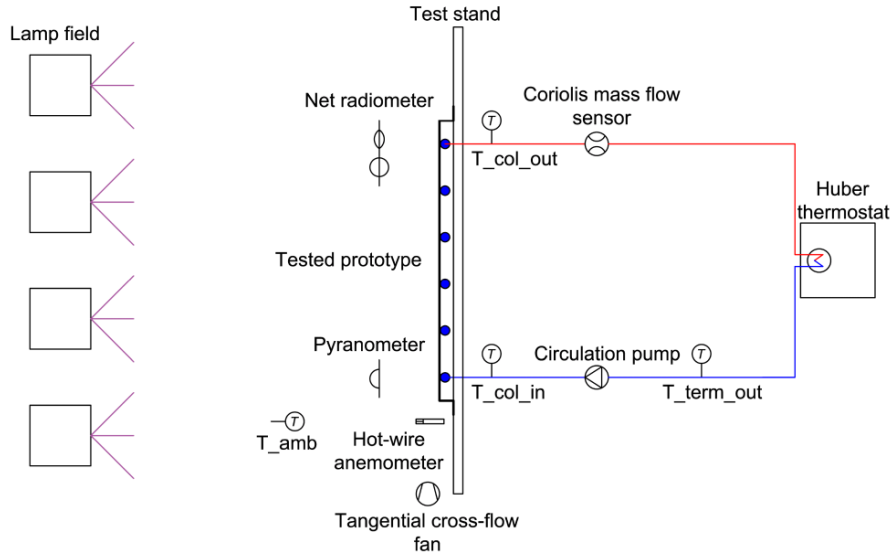

Fig. 6: An indoor solar simulator configuration

Fig. 7: UMFC prototype on the test stand

Tab. 2: The sensors' type and their accuracy

Sensor	Manufacturer	Type	Accuracy
Temperature	TMG	PT100	± 0.05 K
Flow rate	Krohne	Coriolis mass flow sensor OPTIMASS 7000 T10	± 0.002%
Solar irradiation	Kipp & Zonen	Pyranometer SMP1 1 -A	± 1.4%
Long wave irradiation	Kipp & Zonen	CNR4 Net Radiometer	± 4%
Wind velocity	Airflow Lufttechnik GmbH	Hot-wire anemometer D12-65V C	± 0.1 m/s

The prototypes were tested under three wind speeds to obtain steady-state useful thermal output $Q_{c,u}$ for at least three operation points (Fig. 6 and Fig.7). Subsequently, the instantaneous efficiency η_c was determined from Eq. (2) so that

$$\eta_c = \frac{Q_{c,u}}{A_{abs} G"} \qquad \text{(eq. 2)}$$

where $G"$ is the net irradiance at the plane of the collector (W m^{-2}). It was defined from Eq. (3) so that

$$G" = G + \frac{\varepsilon}{\alpha}(E_L - \sigma T_a^4) \qquad \text{(eq. 3)}$$

where E_L is the long wave irradiance in the collector plane (W m^{-2}).

Afterwards, the experimentally obtained useful energy output $Q_{c,u}$ and the analytically calculated instantaneous efficiency η_c were compared with the theoretically calculated characteristics provided by the model. Fig. 8 demonstrates the verification process for prototypes 1 and 3. The verification process for the other UMFC prototypes looks very similar.

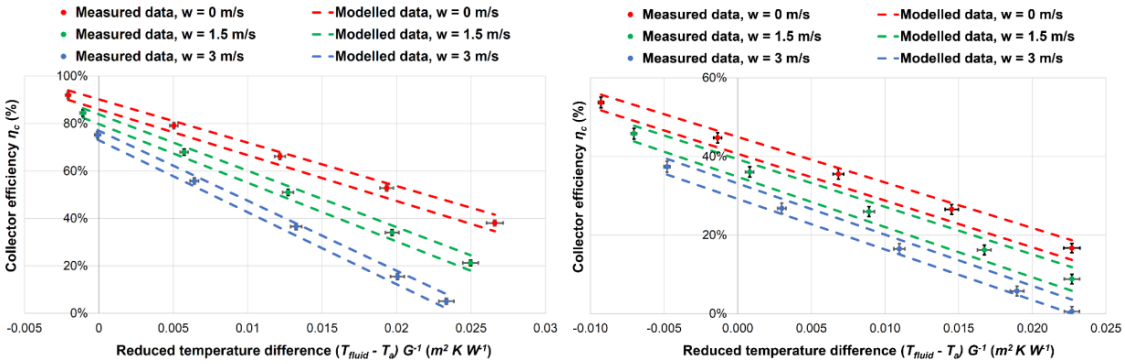

a) b)

Fig. 8: The model verification process for the prototype 1 (a) and the prototype 3 (b)

First of all, it should be noted that the experimentally obtained efficiency points are coupled with the expanded uncertainty points caused by the accuracy of the sensors (see Tab. 2) and the random variation of the measured quantities. Secondly, the theoretically modelled efficiency characteristics the model provides are influenced by the uncertainty of the input design parameters. Therefore, the theoretically calculated efficiency characteristic is presented as an efficiency area. Thirdly, it is worth noting that wind speed substantially influences the thermal performance of the tested UMFC. Finally, comparing and contrasting the experimentally obtained efficiency points and theoretically calculated efficiency area, the modelled results fit the experimentally obtained results relatively well. The flow chart of the verification process is shown in Fig. 9.

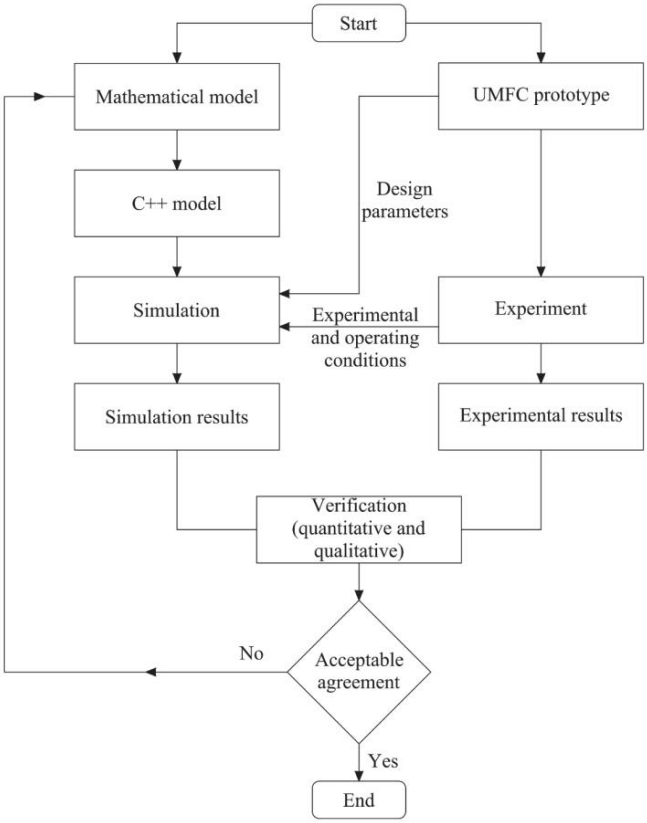

Fig. 9: Flow chart of the verification process

4. Data analysis and the model testing

The thermal performance of a UMFC is significantly affected by heat losses, especially by the front side heat losses. As mentioned above (see Fig. 2), the front side heat losses are caused by two heat transfer processes – by radiation loss from the absorber surface and by combined convection (forced and natural) loss to the ambient. It is evident that due to the relatively low operating temperatures of UMFC, the influence of the radiation heat transfer process is relatively low. On the other hand, the effect of combined convection is significant.

The combined convection heat transfer coefficient is generally calculated as a function of a forced convection heat transfer coefficient using a correlation in terms of wind speed w and natural convection heat transfer coefficient correlation represented by the temperature difference between the surface temperature T_{abs} and the ambient temperature T_a (Eq. 4).

$$h_c = f(h_w(w), h_n(\Delta T)) \qquad \text{(eq. 4)}$$

The present study analyses only the influence of the wind-forced convection model on the theoretically modelled efficiency since wind-induced convective heat transfer has a significantly greater influence than natural convective heat transfer. The issue is that up to now, there is no consensus about an appropriate procedure for the wind-forced convection heat transfer coefficient calculation (Sartori, 2006). As for today, a huge amount of work has been conducted over the last 100 years by different researchers. Palyvos (2008) has presented an exhaustive literature review on the wind-forced convection models, including more than 95 different correlations. This survey includes correlations obtained for façade surfaces and roof-mounted single-glazed solar thermal collectors. Later, Kumar and Mullick (2010) performed experiments for unglazed solar thermal collectors to estimate the wind-caused heat transfer coefficient and compared it with studies of other researchers.

Fig. 10 demonstrates the thermal efficiency area for UMFC prototype 1 with two limiting curves as a result of the proposed mathematical model calculations using 40 different wind-forced convection correlations, which are suitable for unglazed solar thermal collector modelling under the conditions of the performed experiment. First of

all, the modelling results indicate that the theoretically calculated thermal performance is highly dependent on the selection of wind-forced heat transfer correlation used in the model. Secondly, the span of the efficiency area between the limits increases with an increase in wind speed. Therefore, to calculate the thermal performance of a UMFC with a reasonable degree of accuracy, it is extremely important to identify a proper heat transfer correlation for wind-forced convection heat transfer.

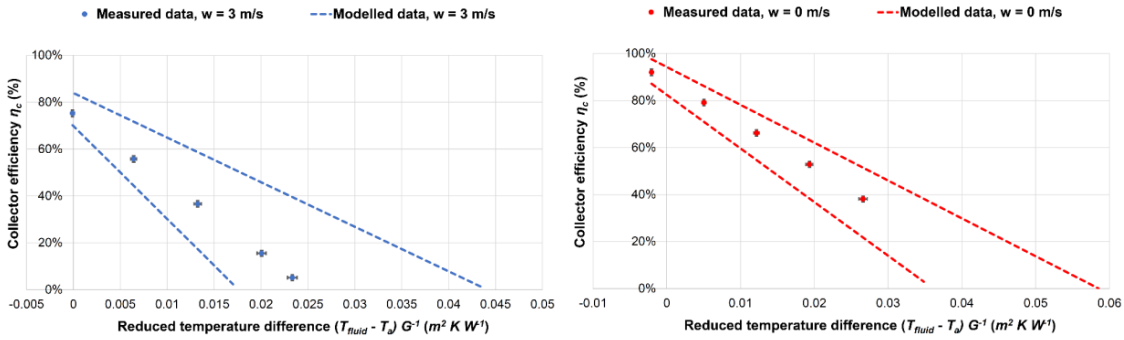

Fig. 10: The thermal efficiency area as a result of the model calculation using 40 suitable wind-forced convection correlations

Fig. 11 presents the efficiency curves as a result of the model calculation for the first UMFC prototype using 5 widely used wind-forced convection correlations (McAdams, 1954; Wattmuff et al., 1977; Test et al., 1981; Kumar et al., 1997; Sharples and Charlesworth, 1998). The simulation results are also compared with the experimental results.

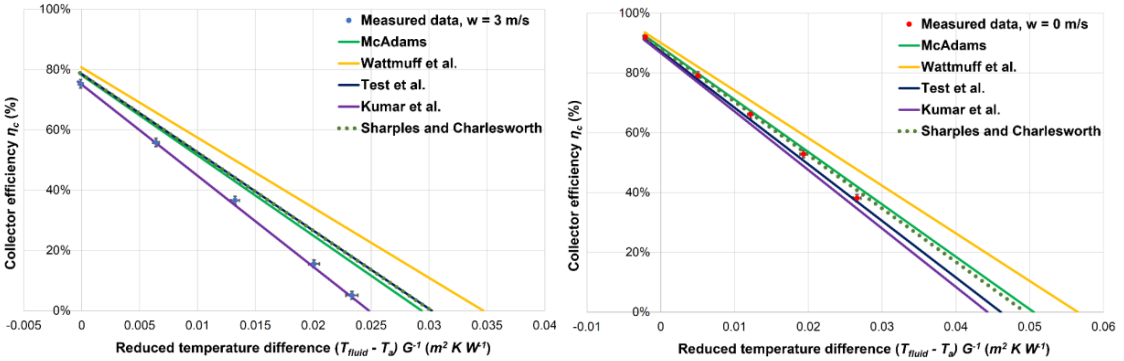

Fig. 11: The thermal efficiency characteristics as a result of the model calculation using 5 widely used wind-forced convection correlations

The simulation results indicate that the wind-forced convection correlations obtained by McAdams (1954) and Wattmuff et al. (1977) give lower values of wind-forced heat transfer coefficient and, consequently, higher efficiency values for the collector. On the other hand, the wind-forced convection correlations obtained by Test et al. (1981) and Sharples and Charlesworth (1998) give higher values of wind-transfer coefficient and, as a result, lower efficiency values. The difference in the simulation results is caused by a difference in the experimental conditions. While McAdams (1954) and Wattmuff et al. (1977) reported their correlations based on wind tunnel measurements, Test et al. (1981) and Sharples and Charlesworth (1998) performed outdoor experiments to obtain wind-forced heat transfer coefficient correlations. The point is that the amount of free stream disturbance in outdoor conditions is generally higher than in wind tunnels at the same speed. Consequently, a higher heat transfer coefficient can be expected in outdoor experiments compared to low turbulence wind tunnel measurement (Test et al., 1981). Moreover, wind flow in a wind tunnel is generally steady, while there are dynamically changing conditions for wind speed and direction during outdoor experiments.

It can also be observed that the experimental results obtained in the present study are somewhat close to the results of Kumar et al. (1997). This may be due fact that the experiment was performed in an indoor environment using an industrial fan. The constant stream disturbance (swirls and turbulence) generated by a large industrial fan can be a factor responsible for higher values of wind-forced convection heat transfer coefficient. Finally, it is evident that the experimental conditions have a crucial influence on the wind-forced heat transfer coefficient and, consequently, on the thermal performance of UMFC prototypes. Therefore, to provide solar system simulation

results with a reasonable degree of accuracy, a long-term outdoor verification process (onsite at best) is highly recommended to find an appropriate wind-forced convection correlation.

5. Conclusion

The paper presents a novel detailed mathematical model of an unglazed metal façade collector. To verify the model, ten differently designed UMFC prototypes were produced based on the conventional metal facade cladding system and experimentally tested. Comparing and contrasting the experimentally obtained efficiency points and theoretically modelled efficiency area span, it can be concluded that the model results fit the experimentally obtained efficiency points sufficiently well.

It was also shown that the thermal performance of a UMFC is greatly influenced by wind-forced convection heat transfer from the front side. Therefore, it is extremely important to identify an appropriate wind-forced convection correlation to minimize the difference between experimentally obtained and theoretically modelled results. Many correlations for wind-forced convection clearly demonstrate that there is no universally acceptable correlation. It is caused by different combinations of experimental conditions (ambient air temperature, wind range, wind tunnel/outdoor/indoor measurement, instrumentation, surroundings, etc.). It should be noted that any wind-forced heat transfer correlation obtained from experimental or analytical results is valid within specific experimental conditions. Actually, Sharples and Charlesworth (1998) and Oliphant (1980) conclusions' agree with this fact and conclude that the results from their work are strictly and only applicable to the particular experimental conditions existing at the site of the measurements. Therefore, the heat transfer model taken from its experimental conditions applied under different conditions leads to incorrect results. Hence, the verification process provided by using an indoor solar simulator in the case of an unglazed solar thermal collector is insufficient. Generally, wind flow under indoor tests is steady, whereas wind is always dynamic in the natural environment as much in wind speed as in wind direction. As a result, a long-term outdoor verification process is highly recommended to find an appropriate wind-forced convection correlation.

Future work will focus on a long-term outdoor verification process based on a large-scale UMFC demonstration under different operation conditions of potential applications (direct hot water preparation, combination with heat pump for hot water preparation and space heating, night cooling, etc.).

6. Acknowledgment

This work was developed within the project Facade system with integrated heat exchanger, CZ.01.1.02/0.0/0.0/20_321/0024470 supported by the Operational Programme Enterprise and Innovations for Competitiveness of the Ministry of Industry and Trade of the Czech Republic. The project is co-financed by the European Union.

7. References

Anderson, T.N., Duke, M., Carson, J.K., 2013. Performance of an unglazed solar collector for radiant cooling.

Bliss Jr., R.W., 1959. The derivations of several "Plate-efficiency factors" useful in the design of flat-plate solar heat collectors. Sol. Energy 3, 55–64. https://doi.org/10.1016/0038-092X(59)90006-4

Bunea, M., Perers, B., Eicher, S., Hildbrand, C., Bony, J., Citherlet, S., 2015. Mathematical modelling of unglazed solar collectors under extreme operating conditions. Sol. Energy 118, 547–561. https://doi.org/10.1016/j.solener.2015.06.012

Eisenmann, W., Mueller, O., Pujiula, F., Zienterra, G., 2006. Metal roofs as unglazed solar collectors, coupled with heat pump and ground storage. Determination of gains from condensation, system concepts; Unverglaste Metalldach-Sonnenkollektoren in Kopplung mit Waeremepumpe und Erdsonde. Bestimmung des Waermeertrag.

Giovanardi, A., Passera, A., Zottele, F., Lollini, R., 2015. Integrated solar thermal façade system for building retrofit. Sol. Energy 122, 1100–1116. https://doi.org/10.1016/j.solener.2015.10.034

Hermann, M., Lunz, K., Hillerns, F., 2010. BIONICOL. Development of a bionic solar collector with an aluminium roll-bond absorber; BIONICOL. Entwicklung eines bionischen Solarkollektors mit Aluminium-Rollbond-Absorber.

Hottel, H., Whillier, A., 1955. Evaluation of flat-plate solar collector performance. Trans. Conf. Use Sol. Energy; 3, 74–104.

Hottel, H., Woertz, B., 1942. Performance of flat-plate solar-heat collectors. Trans. ASME (Am. Soc. Mech. Eng.); (United States) 64, 91–104.

Keller, J., 1985. Characterization of the thermal performance of uncovered solar collectors by parameters including the dependence on wind velocity, humidity and infrared sky radiation as well as on solar irradiance.

Kumar, S., Mullick, S.C., 2010. Wind heat transfer coefficient in solar collectors in outdoor conditions. Sol. Energy 84, 956–963. https://doi.org/10.1016/j.solener.2010.03.003

Kumar, S., Sharma, V.B., Kandpal, T.C., Mullick, S.C., 1997. Wind induced heat losses from outer cover of solar collectors. Renew. Energy 10, 613–616. https://doi.org/10.1016/S0960-1481(96)00031-6

Martinez, R.G., Goikolea, B.A., Paya, I.G., Bonnamy, P., Raji, S., Lopez, J., 2017. Performance assessment of an unglazed solar thermal collector for envelope retrofitting. Energy Procedia 115, 361–368. https://doi.org/10.1016/j.egypro.2017.05.033

McAdams, W.H., 1954. Heat Transmission 3d Ed. McGraw-Hill, New York.

Morrison, G.L., 1994. Simulation of packaged solar heat-pump water heaters. Sol. Energy 53, 249–257. https://doi.org/10.1016/0038-092X(94)90631-9

Morrison, G.L., Gilliaert, D., 1992. Unglazed Solar Collector Performance Characteristics. J. Sol. Energy Eng. 114, 194–200. https://doi.org/10.1115/1.2930005

Oliphant, M. V, 1980. Measurement of wind speed distributions across a solar collector. Sol. Energy 24, 403–405.

Palyvos, J.A., 2008. A survey of wind convection coefficient correlations for building envelope energy systems' modeling. Appl. Therm. Eng. 28, 801–808. https://doi.org/10.1016/j.applthermaleng.2007.12.005

Perers, B., 2010. An improved dynamic solar collector model including condensation and asymmetric incidence angle modifiers, in: EuroSun. 28 September-1 October, 2010 Graz, Austria.

Probst, M.M., Roecker, C., 2007. Towards an improved architectural quality of building integrated solar thermal systems (BIST). Sol. energy 81, 1104–1116.

Sartori, E., 2006. Convection coefficient equations for forced air flow over flat surfaces. Sol. Energy 80, 1063–1071.

Sharples, S., Charlesworth, P.S., 1998. Full-scale measurements of wind-induced convective heat transfer from a roof-mounted flat plate solar collector. Sol. Energy 62, 69–77.

Shemelin, V., Matuska, T., 2022. Unglazed solar thermal collector for building facades. Energy Reports 8, 605–617. https://doi.org/10.1016/j.egyr.2022.07.075

Shen, J., Zhang, X., Yang, T., Tang, L., Wu, Y., Jin, R., Pan, S., Wu, J., Xu, P., 2016. Conceptual Development of a Compact Unglazed Solar Thermal Facade (STF) for Building Integration. Energy Procedia 96, 42–54. https://doi.org/10.1016/j.egypro.2016.09.096

Soltau, H., 1992. Testing the thermal performance of uncovered solar collectors. Sol. Energy 49, 263–272. https://doi.org/10.1016/0038-092X(92)90005-U

Stegmann, M., Bertram, E., Rockendorf, G., Janßen, S., 2011. Model of an unglazed photovoltaic thermal collector based on standard test procedures, in: Proc. of the ISES Solar World Congress. pp. 172–180.

Test, F.L., Lessmann, R.C., Johary, A., 1981. Heat Transfer During Wind Flow over Rectangular Bodies in the Natural Environment. J. Heat Transfer 103, 262–267.

Wattmuff, J.H., Charters, W.W.S., Proctor, D., 1977. Solar and wind induced external coefficients for solar collectors. Coop. Mediterr. pour l'Energie Solaire, Rev. Int. d'Heliotechnique 2, 56.

Weiland, F., Kirchner, M., Rensinghoff, V., Giovannetti, F., Kastner, O., Ridder, D., Tekinbas, Y., Hachul, H., 2019. Performance assessment of solar thermally activated steel sandwich panels with mineral wool core for industrial and commercial buildings. J. Phys. Conf. Ser. 1343, 012098. https://doi.org/10.1088/1742-6596/1343/1/012098

Whillier, A., 1967. Design factors influencing solar collector performance. Low Temp. Eng. Appl. Sol. Energy 27–40.